



COSINUS: Cryogenic Calorimeters for the Direct Dark Matter Search with NaI Crystals

Downloaded from: <https://research.chalmers.se>, 2021-08-31 11:03 UTC

Citation for the original published paper (version of record):

Angloher, G., Carniti, P., Dafinei, I. et al (2020)

COSINUS: Cryogenic Calorimeters for the Direct Dark Matter Search with NaI Crystals

Journal of Low Temperature Physics, 200(5-6): 428-436

<http://dx.doi.org/10.1007/s10909-020-02464-9>

N.B. When citing this work, cite the original published paper.



COSINUS: Cryogenic Calorimeters for the Direct Dark Matter Search with NaI Crystals

G. Angloher¹ · P. Carniti^{2,3} · I. Dafinei⁴ · N. Di Marco⁵ · A. Fuss^{6,7} · C. Gotti^{2,3} · M. Mancuso¹ · P. Martella⁵ · L. Pagnanini^{2,3} · G. Pessina² · F. Petricca¹ · S. Pirro⁵ · F. Pröbst¹ · F. Reindl^{6,7} · K. Schäffner¹ · J. Schieck^{6,7} · D. Schmiedmayer^{6,7} · C. Schwertner^{6,7} · R. Stadler¹ · M. Stahlberg^{6,7} · V. Zema^{5,8,9} · Y. Zhu¹⁰

Received: 21 August 2019 / Accepted: 31 March 2020
© The Author(s) 2020

Abstract

COSINUS (Cryogenic Observatory for Signatures seen in Next-generation Underground Searches) is an experiment employing cryogenic calorimeters, dedicated to direct dark matter search in underground laboratories. Its goal is to cross-check the annual modulation signal the DAMA collaboration has been detecting for about 20 years (Bernabei et al. in *Nucl Part Phys Proc* 303–305:74–79, 2018. <https://doi.org/10.1016/j.nuclphysbps.2019.03.015>) and which has been ruled out by other experiments in certain dark matter scenarios. COSINUS can provide a model-independent test by the use of the same target material (NaI), with the additional chance of discriminating β/γ events from nuclear recoils on an event-by-event basis, by the application of a well-established temperature sensor technology developed within the CRESST collaboration. Each module is constituted by two detectors: the light detector, that is a silicon beaker equipped with a transition edge sensor (TES), and the phonon detector, a small cubic NaI crystal interfaced with a carrier of a harder material (e.g. CdWO₄), also instrumented with a TES. This technology had so far never been applied to NaI crystals because of several well-known obstacles, and COSINUS is the first experiment which succeeded in operating NaI crystals as cryogenic calorimeters. Here, we present the COSINUS project, describe the achievements and the challenges of the COSINUS prototype development and discuss the status and the perspectives of this NaI-based cryogenic frontier.

Keywords Dark matter · Cryogenics · NaI · TES · Phonons · Scintillation · Low-temperature calorimeters

✉ V. Zema
vanessa.zema@gssi.it

Extended author information available on the last page of the article

1 Introduction

During the twentieth century, collecting experimental data to make predictions on a cosmological level has become not only possible, but one of the most powerful tools to probe the Universe. Cosmology and astrophysics provide evidence for the existence of an additional form of matter, whose density is five times larger than that of ordinary matter. This new component of matter is invisible and its nature is unknown; that is why it is called dark matter (DM). Numerous experimental campaigns aiming at direct DM detection are constraining the DM parameter space. Some excesses have been interpreted as positive detection, often not confirmed by the following experimental run. However, this is not the case for the statistically robust result from the DAMA/LIBRA experiment, which has been detecting for about 20 years a signal which is compatible with DM in our galaxy [1]. This is in tension with null results presented as sensitivity curves by other experiments. COSINUS, which employs cryogenic calorimeter working at milli-Kelvin temperature, will provide a cross-check of the DAMA/LIBRA results using the same target material to exclude possible material-dependent effects [2] and will give a decisive answer to this long-standing debate [3–5].

2 Experimental Concept

The COSINUS prototype is a scintillating cryogenic calorimeter operated at milli-Kelvin temperature [6]. The target material is a small cubic NaI crystal installed in a copper housing (Fig. 1, left panel). The detection principle relies on the measurement of the temperature increase caused by an energy deposition in the target material. For this measurement, a temperature sensor is required. COSINUS applies transition edge sensors (TES), a technology developed within the CRESST collaboration. These highly sensitive temperature sensors consist of tungsten thin films (W-TES), whose specifics are described below. If evaporated directly onto

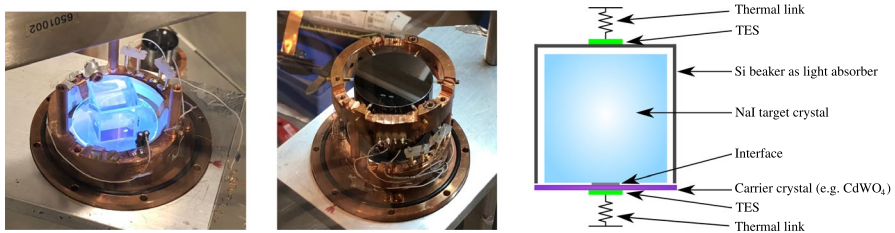


Fig. 1 COSINUS module prototype. Left: Photograph of a NaI crystal and a carrier crystal installed in a copper housing and exposed to UV radiation to show the luminescence effect. Center: Silicon beaker enclosing the NaI crystal, equipped with a transition edge sensor (TES), visible on top of the beaker surface. Right: Schematic drawing of the complete module (color figure online)

the absorber, a good thermal contact can be achieved [7]. However, since NaI is hygroscopic, the evaporation directly on its surface is not feasible.¹ Therefore, the small cube is interfaced with another crystal (e.g. CdWO₄), named carrier, of about 40 mm in diameter and ~ 1 – 2 mm in thickness, which is instrumented with a TES instead. The interface between NaI and carrier is made of amorphous materials, like epoxy resin or silicone oil. Energy depositions in the target material cause lattice vibrations whose energy flux is transmitted to the carrier and measured by the TES as an increase in temperature. The NaI crystal, interfaced with the carrier and the TES, is the phonon detector. The detected scintillation light, which accounts for about 10% with respect to the energy converted into heat, is measured by a beaker-shaped light absorber made from silicon and enclosing the NaI target. The silicon beaker dimensions are: 40 mm in diameter, 39 mm in height and a wall-thickness of about 420 μm. Its mass is about 9 g. It is produced by Optec² and is machined from bulk silicon, by using a hole saw cutter drill. The surfaces are polished to optical quality. The silicon beaker is also instrumented with a TES (Fig. 1, central panel). The silicon beaker and the carrier disk are designed to optimise the active surrounding coverage of the target material, in order to fight the surface α -induced background, whose back-to-back emission can produce a nuclear recoil analogous to the expected DM signal. The silicon beaker, equipped with the TES, is the light detector.

The W-TES (thickness of 200 nm) is evaporated on the carrier and operated in its transition from normal to superconducting state, commonly around 15–20 mK. An energy deposition results in a temperature increase, which can be measured by the resistance change of the TES—the steeper the transition, the more sensitive the TES. The TES resistance works as electric component of a readout circuit, and the output voltage is finally registered by SQUID (Superconducting Quantum Interference Device) amplifiers. The W-TES technology used here was pushed within CRESST to a sensitivity level of about 4.6 eV baseline resolution (σ) for a 24 g CaWO₄ crystal (CRESST-III) [8].

The dual-channel readout of heat and light is a powerful tool for particle discrimination, since the amount of deposited energy going into the production of light depends on the type of event. The suppression expected for nuclear scatterings and α -events with respect to β/γ -events is called light quenching. The ratio between the amount of energy going into light and the amount of energy converted into heat allows for particle discrimination.

¹ Photolithography and handling NaI in electron-beam evaporation systems and sputter machines are not feasible for guaranteeing both a controlled humidity-free atmosphere and temperature far away from the melting point.

² <https://www.optec-muenchen.de/>.

3 Status of the Prototype Development

Improving the radio-purity of NaI crystals is an important step of the COSINUS prototype development. For what concerns potassium concentration, achieving high radio-purity is crucial because of the ^{40}K -decay emission, which is a source of background in the region of interest of DAMA. In collaboration with SICCAS (Shanghai Institute of Ceramics, Chinese Academy of Science), COSINUS achieved the result of growing NaI crystals with potassium concentrations of 5–9 ppb at crystals' nose and 22–35 ppb at crystals' tail [9]. COSINUS crystals' potassium concentration at the crystals' nose is below the one of DAMA crystals.

With the beaker-shaped light-absorber design, $\sim 13\%$ ($\sim 10\%$) of the energy deposited in pure (doped) NaI crystals is measured in the light detector [10]. The light-energy threshold achieved is $\sim 0.6 \text{ keV}_{ee}$ (electron equivalent). The phonon-energy threshold is still far from the COSINUS goal of 1 keV,³ although it has been improved with respect to the threshold reached in [10] that was $\sim 8.26 \text{ keV}$ (the best recent prototypes arrive at 5–6 keV). The challenging phonon-threshold optimisation is attributed to the vibrational properties of NaI, which require an accurate choice of the temperature sensor (e.g. TES/NTD and geometry) and of the general detector design (e.g. carrier material).

3.1 Studies on Pulse Formation

Both theoretical and experimental studies on the pulse formation in a COSINUS-like detector set-up are ongoing. From the theory side, the effort is twofold: (1) writing down a system of equations which describes the time dependence of the TES response as function of all the thermal couplings involved and (2) studying the vibrational properties of the NaI lattice to predict reasonable values for the parameters of the model.

Modelling of the TES response Results on pulse shape analysis from the first NaI detector run [11] (see [12] for preliminary studies on CsI, which anticipated the COSINUS project) are based on [13]. The model in [13] refers to bolometric detectors working in a scheme similar to the one of COSINUS, but without the carrier. This model was used for a CRESST detector with a carrier [14] and provided a good description of the detector response [15]. For this reason, it was also used for the COSINUS module. The solution of the system of equations describing the time-dependent response of an ideal temperature sensor $T_e(t)$ ⁴, is,⁵

³ Note that in the phonon channel, the energy threshold is already a nuclear recoil energy threshold. As comparison, in DAMA/LIBRA, the threshold of $\sim 1 \text{ keV}_{ee}$ corresponds to $\sim 3 \text{ keV}$ in a recoil off Na, for a light-quenching factor of ~ 0.3 , and to $\sim 10 \text{ keV}$ in a recoil off I, for a light-quenching factor of ~ 0.1 .

⁴ Equation 1 neglects the finite thermal conductance along the film; that is why the sensor is 'ideal'. In [13], also the realistic case which considers the finite thermal conductance along the film is discussed and solved. The explicit dependence on the physical parameters involved (conductances, heat capacity, power input, ...) is also given there.

⁵ Equation 1 is the solution of the differential system in Eqs. 8–9 of [13] if the amplitude A_n in Eq. 12 of [13] is corrected by a minus sign overall.

$$T_e(t) - T_b = \Delta T_e(t) = A_n(e^{-t/\tau_n} - e^{-t/\tau_{in}}) + A_t(e^{-t/\tau_t} - e^{-t/\tau_n}) \quad (1)$$

where T_b is the temperature of the thermal bath, A_n and A_t are interpreted as the amplitudes of the nonthermal and the thermal components, τ_{in} and τ_t are the time constants of the sensor response and the relaxation time of thermal component in the absorber, respectively. τ_n is the characteristic relaxation time of athermal phonons, depending on the properties of the crystal and of the film, which reads,

$$\tau_n = \left(\frac{1}{\tau_{\text{film}}} + \frac{1}{\tau_{\text{crystal}}} \right)^{-1} \quad (2)$$

where τ_{film} and τ_{crystal} are the thermalisation time constants in the thermometer and in the crystal, respectively.

The model from Eq. 1 was used to fit COSINUS experimental data [11], but was found insufficient to describe the pulse shape. In [11], a second thermal component was added to obtain reasonable results (see Table 1 of [11]). As anticipated above, Eq. 1 solves a system of equations which do not include the carrier. The first modification to implement is to consider the carrier and find the solution of the complete system. This calculation is ongoing.

Studies on vibrational properties of NaI lattice The optimisation of COSINUS detectors requires a careful study of the vibrational properties of the NaI lattice, to identify the whole system working regime and plan the prototype optimisation accordingly. The detector performance is strictly related to the ratio of the time constants τ_n and τ_{in} . This ratio establishes the relation between the sensor response and the vibrational properties of the target material, because the ratio depends on τ_{crystal} , as shown in Eq. 2. The ongoing derivation of the complete model for COSINUS detectors will allow the estimation of τ_{crystal} as data-fit parameter. On the other hand, a simulation of the microscopic behaviour of NaI crystals will support and validate the results of the parameter estimation performed by data analysis. To this aim, the solid-state theoretical group of the University of L'Aquila has been involved.

4 Quenching Factor Measurement

According to Birks' law [16], the amount of scintillation light emitted due to the scattering of a particle off a scintillating material decreases as the mass of the scattered particle increases. The ratio between the amount of light emitted following the interaction of a particle in the crystal and the amount of light emitted after a β/γ interaction of the same energy is the quenching factor (QF) for that type of particle. Since the quenching factors may depend on different properties, such as the temperature, the crystal doping or the concentration of impurities or defects of the lattice [17, 18], a dedicated QF measurement for COSINUS crystals is mandatory. Low-temperature QF measurements can be done via calibration with radioactive neutron sources as well as via calibration with a mono-energetic neutron beam at accelerator facilities. Besides neutron calibration campaigns at LNGS, COSINUS already ran two measurements at the Maier-Leibnitz Laboratorium, (facility now

indefinitely closed) one on a NaI(pure) crystal in April 2018, and one on a NaI(Tl) crystal, in November 2018, and the data analyses are ongoing.

To quantify the influence of the level of thallium (Tl) dopant on the quenching factors, a systematic study of the performance of NaI crystals with different thallium concentrations and at different temperatures is planned. Crystals with different amounts of Tl dopant (200 ppm, 500 ppm, 1000 ppm, 1500 ppm) will be operated both as cryogenic detectors using an AmBe neutron source and as scintillation detectors at room temperature, at the Triangle University Nuclear Laboratory (TUNL) scattering facility, USA, using a neutron beam.

5 Status of the Experimental Site

The COSINUS experiment will be hosted in LNGS—Laboratori Nazionali del Gran Sasso, Italy. The project for the construction is in preparation. The background budget evaluation and the shielding concept were investigated using GEANT4 simulations (results to be published). The project foresees a 7×7 m water tank, surrounding the dry well hosting the cryostat (Fig. 2). The shielding configuration which minimises the background level is described in Table 1. With about 2m of water thickness, the number of surviving ambient neutrons expected to reach the detector volume is $\sim 10^{-8} \text{ kg}^{-1} \text{ yr}^{-1}$. With the shielding configuration described in Table 1, the number of total (steel+Cu) radiogenic neutrons reaching the detector volume with $E > 1 \text{ keV}$ is found to be $3.08 \times 10^{-3} \text{ kg}^{-1} \text{ yr}^{-1}$, while the number of cosmogenic neutrons caused by muon interactions in the rock and in the shielding material is expected to be $7.44 \times 10^{-1} \text{ kg}^{-1} \text{ yr}^{-1}$. Since the cosmogenic contribution is found to be two orders of magnitude larger than the radiogenic background level, an active muon veto is planned.

The water tank will be used as an active Cherenkov veto. An optical simulation was performed to establish the optimal configuration and operation for PMTs. An efficient muon veto system can be obtained by using ~ 18 – 28 PMTs and defining a fivefold PMT coincidence with a trigger on the single photoelectron within a time window of a few 100 ns. A refined configuration for both the background shielding and the muon veto system will be defined in the near future, according to the results of the experimental measurements.

6 Conclusion

COSINUS will provide a model-independent cross-check of the DAMA/LIBRA results. The prototype performance was pushed to a light-energy threshold of 0.6 keV_{ee} . The phonon-channel threshold of $\sim 8.26 \text{ keV}$ is planned to be improved by studying in more depth the vibrational properties of the NaI crystal lattice and adjusting the layout of the temperature sensors accordingly. The best recent prototypes arrive at 5 – 6 keV ; COSINUS' goal is to reach 1 keV . The crystals

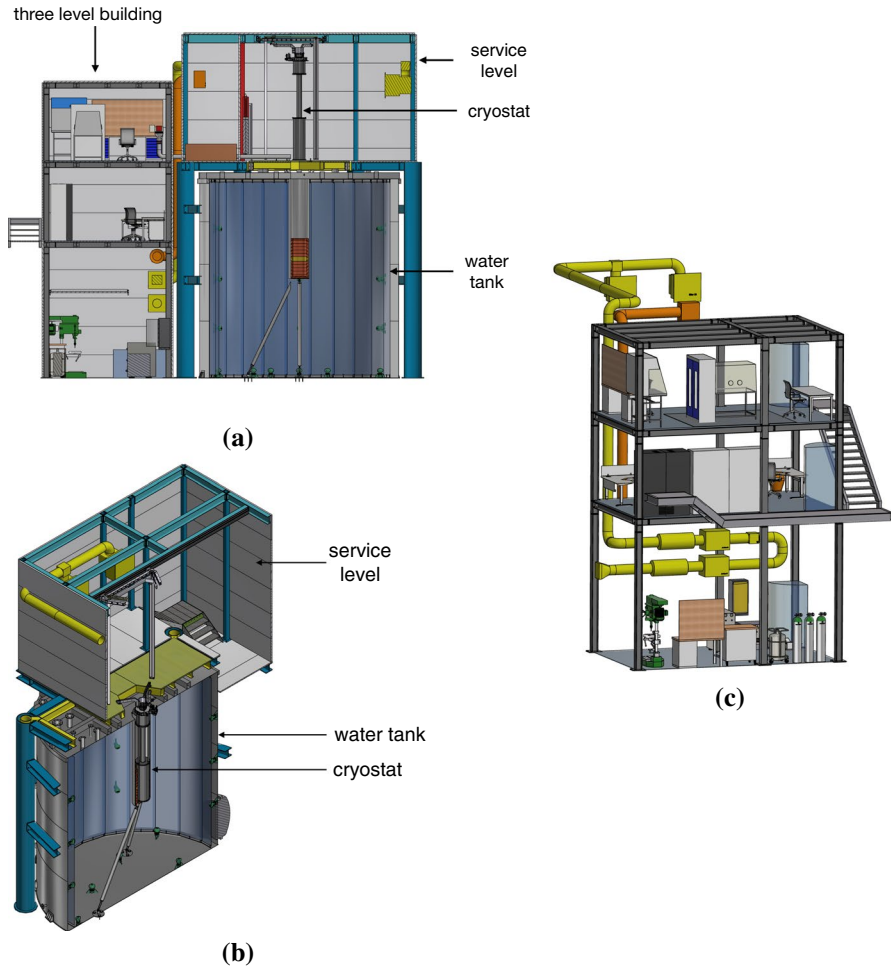


Fig. 2 The scheme shows a preliminary 3D section of the COSINUS experimental set-up as located in hall B of LNGS. The cryostat hosting the COSINUS detectors is inserted in the dry well of a 7×7 -m water tank. Panel **a**: the cryostat lifted up from the dry well to the servicing level. The servicing level equipped with a clean room allows for detector mounting. The three-level building close to the water tank will host the DAQ and the electronics, the cryostat-related infrastructure and a working area. Panel **b**: sectional view of the cryostat inserted in the dry well of the water tank and, on top of the water tank, the service level. Panel **c**: 3D view of the three-level control building (color figure online)

Table 1 Measures for the shielding configuration, featuring the optimal thicknesses of water, Pb, Cu and PE

Tank (stainless) (cm)	Water radius (cm)	Dry well (stainless) (cm)	Pb (cm)	Cu (cm)	PE (cm)	Cryostat (Cu) (cm)	Top shield Pb + Cu + PE (cm)
1.5	300	0.4	0	8	0	0.8	0 + 30 + 0

developed at SICCAS already exceed the aimed-for-radio-purity goal. Quenching factor measurements studying the impact of Tl dopant on scintillation light emission at both room and low temperatures are planned. The construction of the COSINUS experimental facility, designed according to dedicated GEANT4 simulations for background suppression, is in progress. Together with finalising the detector design until 11/2020, COSINUS would then be ready for data taking in 11/2021 and first dark matter results with 100 kg days of exposure could be expected for 02/2023.

Acknowledgements Open access funding provided by Chalmers University of Technology. The COSINUS Collaboration acknowledges the LNGS mechanical workshop team E. Tatanni, A. Rotilio, A. Corsi and B. Romualdi for their continuous contribution to the set-up construction, M. Guetti for his essential technical support and the LNGS technical division, with technical coordinator S. Gazzana, for the realisation of the project.

Open Access This article is licensed under a Creative Commons Attribution 4.0 International License, which permits use, sharing, adaptation, distribution and reproduction in any medium or format, as long as you give appropriate credit to the original author(s) and the source, provide a link to the Creative Commons licence, and indicate if changes were made. The images or other third party material in this article are included in the article's Creative Commons licence, unless indicated otherwise in a credit line to the material. If material is not included in the article's Creative Commons licence and your intended use is not permitted by statutory regulation or exceeds the permitted use, you will need to obtain permission directly from the copyright holder. To view a copy of this licence, visit <http://creativecommons.org/licenses/by/4.0/>.

References

1. R. Bernabei et al., Nucl. Part. Phys. Proc. **303–305**, 74–79 (2018). <https://doi.org/10.1016/j.nuclphysbps.2019.03.015>
2. F. Kahlhoefer et al., JCAP **1805**, 074 (2018). <https://doi.org/10.1088/1475-7516/2018/05/074>
3. G. Adhikari et al., Eur. Phys. J. C **78**(2), 107 (2018). <https://doi.org/10.1140/epjc/s10052-018-5590-x>
4. J. Amaré et al., Phys. Rev. Lett. **123**(3), 031301 (2019). <https://doi.org/10.1103/PhysRevLett.123.031301>
5. C. Tomei et al., Nucl. Instrum. Meth. A **845**, 418 (2017). <https://doi.org/10.1016/j.nima.2016.06.007>
6. G. Angloher et al., Eur. Phys. J. C **76**, 441 (2016). <https://doi.org/10.1140/epjc/s10052-016-4278-3>
7. W. Seidel, G. Forster, W. Christen, F. Von Feilitzsch, H. Gobel, F. Probst, R.L. Mossbauer, Phys. Lett. B **236**, 483 (1990). [https://doi.org/10.1016/0370-2693\(90\)90388-M](https://doi.org/10.1016/0370-2693(90)90388-M)
8. A.H. Abdelhameed et al., Phys. Rev. D **100**(10), 102002 (2019). <https://doi.org/10.1103/PhysRevD.100.102002>
9. Y. Zhu et al., *Proceedings, IEEE Nuclear Science Symposium and Medical Imaging Conference (NSSMIC 2018)*, <https://doi.org/10.1109/NSSMIC.2018.8824322>
10. K. Schäffner et al., J. Low. Temp. Phys. **193**(5–6), 1174 (2018). <https://doi.org/10.1007/s10909-018-1967-3>
11. G. Angloher et al., JINST **12**, P11007 (2017). <https://doi.org/10.1088/1748-0221/12/11/P11007>
12. G. Angloher et al., *Astropart. Phys.* **84**, 70–77, <https://doi.org/10.1016/j.astropartphys.2016.08.005>
13. F Probst et al., J. Low. Temp. Phys. **100**, no 69–104 (1995) <https://doi.org/10.1007/BF00753837>
14. G. Angloher et al., Eur. Phys. J. C **76**, no 1 (2016) <https://doi.org/10.1140/epjc/s10052-016-3877-3>
15. F. Reindl, Munich Tech. U. PhD Thesis (2016) <http://www.mediatum.ub.tum.de/id=1294132>
16. J.B. Birks, *International series of Monographs on Electronics and Instrumentation*, vol. 27 (Macmillan, New York, 1964)

17. V.I. Tretyak, *Astropart. Phys.* **33**, 40 (2010). <https://doi.org/10.1016/j.astropartphys.2009.11.002>
18. V.I. Tretyak, *EPJ Web Conf.* **65**, 02002 (2014). <https://doi.org/10.1051/epjconf/20136502002>

Publisher's Note Springer Nature remains neutral with regard to jurisdictional claims in published maps and institutional affiliations.

Affiliations

G. Angloher¹ · P. Carniti^{2,3} · I. Dafinei⁴ · N. Di Marco⁵ · A. Fuss^{6,7} · C. Gotti^{2,3} · M. Mancuso¹ · P. Martella⁵ · L. Pagnanini^{2,3} · G. Pessina² · F. Petricca¹ · S. Pirro⁵ · F. Pröbst¹ · F. Reindl^{6,7} · K. Schäffner¹ · J. Schieck^{6,7} · D. Schmiedmayer^{6,7} · C. Schwertner^{6,7} · R. Stadler¹ · M. Stahlberg^{6,7} · V. Zema^{5,8,9} · Y. Zhu¹⁰

¹ Max-Planck-Institut für Physik, 80805 Munich, Germany

² INFN - Sezione di Milano Bicocca, 20126 Milan, Italy

³ Dipartimento di Fisica, Università di Milano-Bicocca, 20126 Milan, Italy

⁴ INFN - Sezione di Roma 1, 00185 Rome, Italy

⁵ INFN - Laboratori Nazionali del Gran Sasso, 67010 Assergi, Italy

⁶ Institut für Hochenergiephysik der Österreichischen Akademie der Wissenschaften, 1050 Wien, Austria

⁷ Atominstitut, Technische Universität Wien, 1020 Wien, Austria

⁸ Gran Sasso Science Institute, 67100 L'Aquila, Italy

⁹ Chalmers University of Technology, SE-412 96 Göteborg, Sweden

¹⁰ SICCAS - Shanghai Institute of Ceramics, Shanghai, People's Republic of China